Dynamics of Energy Transfer from Lycopene to Bacteriochlorophyll in Genetically-Modified LH2 Complexes of *Rhodobacter sphaeroides*†

H. Hörvin Billsten,‡ J. L. Herek,‡ G. Garcia-Asua,§ L. Hashøj,‡ T. Polívka,‡ C. N. Hunter,§ and V. Sundström*,‡

Department of Chemical Physics, Lund University, P.O. Box 124, S-22100 Lund, Sweden, and Krebs Institute for Biomolecular Research and Robert Hill Institute for Photosynthesis, Department of Molecular Biology and Biotechnology, University of Sheffield, Sheffield S10 2TN, U.K.

Received August 31, 2001; Revised Manuscript Received December 13, 2001

ABSTRACT: LH2 complexes from *Rb. sphaeroides* were modified genetically so that lycopene, with 11 saturated double bonds, replaced the native carotenoids which contain 10 saturated double bonds. Tuning the S_1 level of the carotenoid in LH2 in this way affected the dynamics of energy transfer within LH2, which were investigated using both steady-state and time-resolved techniques. The S_1 energy of lycopene in *n*-hexane was determined to be $\sim$12 500 $\pm$ 150 cm^{-1}, by direct measurement of the S_1-S_2 transient absorption spectrum using a femtosecond IR-probing technique, thus placing an upper limit on the S_1 energy of lycopene in the LH2 complex. Fluorescence emission and excitation spectra demonstrated that energy can be transferred from lycopene to the bacteriochlorophyll molecules within this LH2 complex. The energy-transfer dynamics within the mutant complex were compared to wild-type LH2 from *Rb. sphaeroides* containing the carotenoid spheroidene and from *Rs. molischianum*, in which lycopene is the native carotenoid. The results show that the overall efficiency for Crt → B850 energy transfer is $\sim$80% in lyco-LH2 and $\sim$95% in WT-LH2 of *Rb. sphaeroides*. The difference in overall Crt → BChl transfer efficiency of lyco-LH2 and WT-LH2 mainly relates to the low efficiency of the Crt S_1 → BChl pathway for complexes containing lycopene, which was 20% in lyco-LH2. These results show that in an LH2 complex where the Crt S_1 energy is sufficiently high to provide efficient spectral overlap with both B800 and B850 Q_y states, energy transfer via the Crt S_1 state occurs to both pigments. However, the introduction of lycopene into the *Rb. sphaeroides* LH2 complex lowers the S_1 level of the carotenoid sufficiently to prevent efficient transfer of energy to the B800 Q_y state, leaving only the Crt S_1 → B850 channel, strongly suggesting that Crt S_1 → BChl energy transfer is controlled by the relative Crt S_1 and BChl Q_y energies.

The peripheral LH2[1] light-harvesting complex is part of the photosynthetic unit of many species of purple bacteria. The crystal structure of LH2 from *Rhodopseudomonas (Rps.) acidophila* has been resolved to 2.5 Å (*1*) and is found to consist of nine repeating protein−pigment units forming two concentric rings with C_9 symmetry. Overall, 27 bacteriochlorophylls (BChls) and nine carotenoid molecules (rhodopsin glucoside) are contained within the protein scaffold. Eighteen of the BChls are in close contact with each other and are labeled B850 after their maximal absorption at 850 nm. The nine "monomeric" BChls have a peak absorption wavelength at 800 nm and are therefore referred to as B800. When studying the crystal structure, one can see that the carotenoids are in close contact with both the B800 and the B850 BChl molecules. The structure of the LH2 of *Rhodospirillum (Rs.) molischianum* has also been investigated; it has a similar organizational motif (see Figure 1) and possesses C_8 symmetry (*2*).

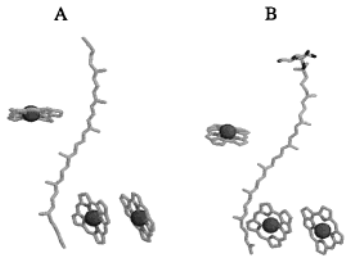

FIGURE 1: Organization of pigments in the subunit of LH2 of (A) *Rps. acidophila* and (B) *Rs. molischianum*. In *Rps. acidophila*, this subunit is repeated 9 times to form a symmetric ring structure (C_9), and the carotenoid is rhodopin glucoside (have shown without glucoside ring). The LH2 from *Rs. molischianum* possesses C_8 symmetry, and the carotenoid is lycopene. Another difference between the LH2 complexes is that the plane of the B800 molecules in *Rs. molischianum* is rotated 90° compared to *Rps. acidophila*. Electron microscopy shows that the LH2 of *Rb. sphaeroides* is similar to that of *Rps. acidophila* although it does not show perfect C_9 symmetry, which depends on a small tilt of the individual rings of LH2 relative to the membrane (*6*).

† This work was supported by the Swedish Natural Science Research Council and the Knut and Alice Wallenberg Foundation. G.G.-A. was supported by a grant from the European Union (Grant ERBFMGECT-950020). G.-G.A. and C.N.H. were supported by a grant from the BBSRC (U.K.).

* Corresponding author. Tel.: +46-46-2224690; Fax: +46-46-2224119; E-mail: villy.sundstrom@chemphys.lu.se.

‡ Lund University.

§ University of Sheffield.

[1] Abbreviations: BBO, beta barium borate; BChl, bacteriochlorophyll; ESA, excited-state absorption; Crt, carotenoid; DNA, deoxyribonucleic acid; EDTA, ethylenediaminetetraacetate; fwhm, full width at half-maximum; HPLC, high-performance liquid chromatography; ICM, intracytoplasmic membrane; LH, light harvesting; LH1, core light-harvesting complex; LH2, peripheral light-harvesting complex; lyco-LH2, genetically modified LH2 containing lycopene; PCR, polymerase chain reaction; *Rb.*, *Rhodobacter*; RC, reaction center; *Rps.*, *Rhodopseudomonas*; *Rs.*, *Rhodospirillum*; WT, wild-type.

10.1021/bi011741v CCC: $22.00
Published on Web 02/22/2002

The structural data for these LH2 complexes have opened new possibilities for detailed studies of their structure−function relationships. This is because the wealth of structural data on LH2 complexes is matched by the amount of steady-state and kinetic information on the spectroscopic properties of these molecules (*3*). In addition, the complex from *Rhodobacter (Rb.) sphaeroides* offers the possibility of genetic manipulation, which can be used selectively to alter residues involved in modifying the spectroscopic properties of the bacteriochlorophylls within LH2 (*4, 5*). Cryo-electron microscopy of this complex has revealed that it is composed of a nine-membered ring, as for the *Rps. acidophila* complex (*6*). Thus, the LH2 complex has become widely regarded as a prototype system for studies of interpigment and pigment−protein couplings, dynamics, and aggregate effects (*3*), since it offers a relatively simple structure, featuring well-ordered arrays of pigment molecules embedded in an organized protein scaffold.

Considerable interest has focused on elucidating the mechanism of energy transfer between BChl molecules as well as between carotenoids and BChls. Obtaining a detailed picture of the energy transfer of LH2 is a difficult task because of the many different pathways that may be involved. Excitation transfer among the BChl molecules of LH2 has been characterized in great detail with the help of ultrafast spectroscopy and has been correlated with the structure of LH2 to yield insight into the function of the complex (*3*). However, to date there is no general description of how energy is transferred between carotenoids and bacteriochlorophylls in LH2, although it seems that the excitation energy can be transferred to both B800 and B850 molecules (*7*−*9*).

The basis of carotenoid function in LH2 is the unusual photophysics of carotenoid molecules. Carotenoids possess two low-lying electronic states, S_1 and S_2, both playing important roles in the energy-transfer processes. An electronic transition between the ground state and the lowest excited state, S_1, is symmetry-forbidden because they both possess A_g symmetry in the idealized C_{2h} point group of polyenes. However, the transition between the ground state and the second excited state, S_2, which has B_u symmetry, is strongly allowed, and this transition is responsible for the characteristic strong absorption associated with carotenoids in the visible spectral region. Despite the fact that the S_0−S_1 transition is forbidden, the S_1 state can be populated via optical excitation of S_2, followed by ultrafast internal conversion. The S_1 state has a lifetime ranging from a few to hundreds of picoseconds, depending on the number of conjugated C═C bonds in the carotenoid (*10*), and because of the forbidden nature of this state, the S_1 fluorescence yield of naturally occurring carotenoids is very low (*11*).

Early transient absorption measurements on the LH2 complex of *Rb. sphaeroides* (*12, 13*) indicated that energy is transferred from the initially excited Crt S_2 state along two competing pathways: direct transfer to the BChls and transfer to the BChls via the Crt S_1 state. Fluorescence up-conversion experiments on the B800−820 LH2 complex of *Rps. acidophila* (*14*) and *Rb. sphaeroides* (*15*) LH2 substantiated these suggestions and demonstrated the presence of a fast channel (65−130 fs) for energy transfer from the Crt S_2 state to B820. It was suggested that this energy-transfer pathway involves direct transfer from the Crt S_2 state to the BChl Q_x state. From the same work (*14, 15*), Crt S_1 to BChl Q_y energy transfer was suggested to occur on the ∼10 ps time scale. Similar conclusions were drawn from transient absorption measurements on the B800−B830 light-harvesting complex of *Chromatium purpuratum* (*16*). These authors suggested a model in which one okenone carotenoid molecule is coupled to B830 and mainly transfers energy along the Crt S_2 − B830 Q_x pathway. Another okenone molecule was suggested to be coupled to B800 and transfer energy along the Crt S_2 − Crt S_1 − B800 Q_y path.

From these initial time-resolved studies, it appeared that carotenoid to BChl energy transfer in LH2 follows a complex pattern where all the low-lying excited states of all pigments are involved. However, no general scheme or mechanisms of energy transfer could be discerned. Several recent studies have explicitly addressed the energy transfer from the Crt S_1 state. By reconstituting LH2 of *Rb. sphaeroides* with carotenoids having 7−13 conjugated double bonds, Frank and co-workers (*17*) found that carotenoids having 10 or fewer C═C bonds transfer energy to the BChl molecules via their S_1 states. They also found that energy transfer via the S_2 state is more important as the number of C═C bonds increases.

In a similar study, Koyama and co-workers addressed the mechanism of the Crt S_1 − BChl Q_y transfer by studying the rate and efficiency of Crt S_1 to BChl Q_y energy transfer in LH2 reconstituted with three different carotenoids: lycopene (11 double bonds), spheroidene (10 double bonds), and neurosporene (9 double bonds) (*10*). It was concluded that both the rate and efficiency of Crt S_1 − BChl, as well as the efficiency of overall Crt − BChl energy transfer, increase with decreasing conjugation length of the carotenoid. The mechanism of energy transfer from the Crt S_1 state was suggested to be mainly of Coulombic origin through intensity borrowing of the S_1 state from the strongly dipole-allowed Crt S_2 state.

Another approach to study energy transfer via the S_1 state in LH2 of *Rps. acidophila* and *Rb. sphaeroides* was used by Walla et al. (*18*): the Crt S_1 state was directly populated by two-photon absorption and its decay monitored by probing the S_1−S_n transition of the carotenoid. The advantage of two-photon excitation is that it is possible to excite the S_1 state directly and this enables measurements without contribution from the optically allowed S_2 state. It was concluded that for LH2 of *Rps. acidophila* the Crt S_1 − BChl energy transfer is rather inefficient (28%) with a B800:B850 ratio of 40:60, while in *Rb. sphaeroides* LH2 the transfer is much more efficient (80%) with a B800:B850 ratio of 85:15.

Recently, fluorescence up-conversion experiments performed by Gillbro et al., on the B800−B850 LH2 complexes from *Rps. acidophila*, showed that the overall efficiency of energy transfer from the carotenoid (rhodopsin glucoside) S_1 and S_2 states to BChl is 56% and the most efficient process is from the S_2 state of the carotenoid to the BChl B850 molecules (31%). This work also showed that the B800 molecules receive energy primarily from the Crt S_2 state (20%), but a very small amount (5%) comes from the S_1 state. Further, their results show that no energy transfer occurs between the S_1 state and the B850 BChl molecules (*19*).

The creation of a new mutant of *Rb. sphaeroides* containing the carotenoid lycopene (11 conjugated double bonds) has formed the basis of the experiments reported here. By

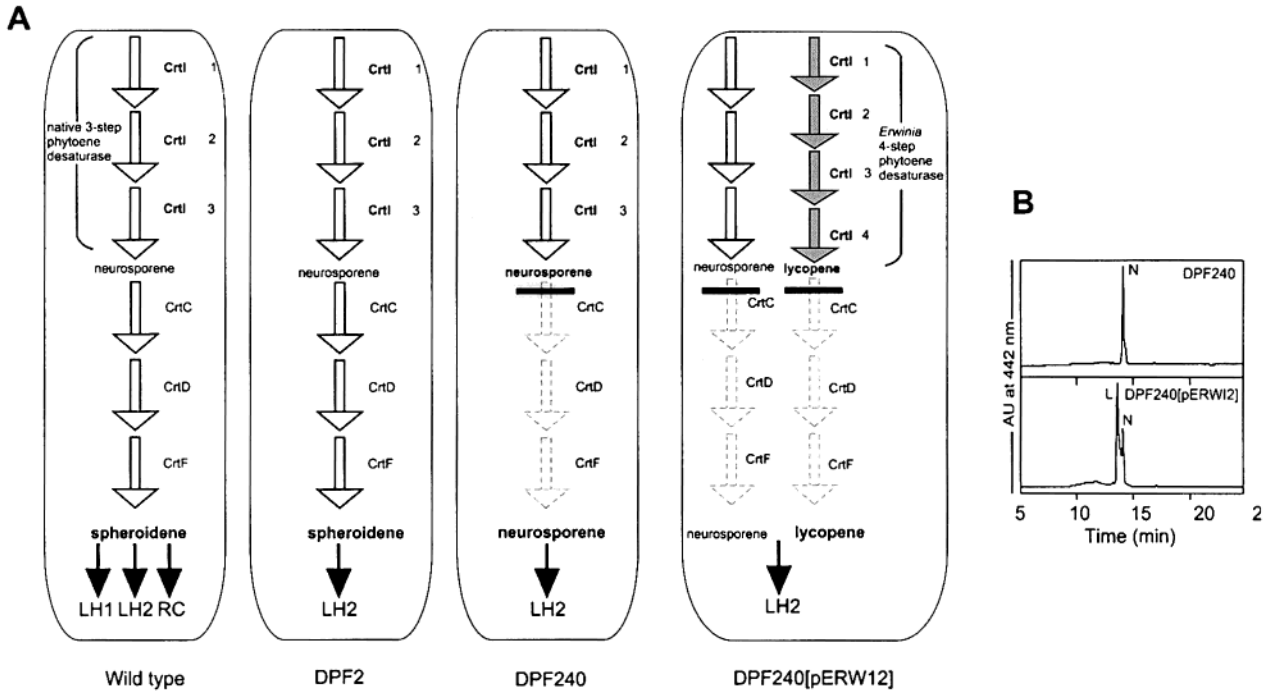

FIGURE 2: (A) Scheme depicting the effects of the genetic manipulations involved in the carotenoid biosynthetic pathway of *Rb. sphaeroides*. The wild-type strain produces LH2, LH1, and RC complexes containing spheroidene/spheroidenone as the native carotenoids. Genetic manipulation (*22*) results in the LH2-only strain DPF2. Insertion of transposon Tn*5* in the *crt*C gene of DPF2 stops the pathway prematurely, and neurosporene accumulates, which is incorporated into LH2. Finally, plasmid pERWI2, containing the *Erwinia crtI* gene, was introduced by conjugative transfer into mutant DPF240. The 4-step phytoene desaturase encoded by the *Erwinia crtI* gene allows the biosynthetic pathway to progress from neurosporene (3 desturations) to lycopene (4 desaturations). (B) HPLC analysis of carotenoid content of the DPF240 and DPF240[pERWI2] strains. In the latter strain, lycopene forms 80% of the carotenoid present, and neurosporene 20%.

genetically incorporating lycopene, the carotenoid native to *Rs. molischianum*, into the LH2 complex of *Rb. sphaeroides*, a number of aspects could be addressed. One aspect concerns whether a carotenoid that is normally operative in an eight-membered ring also can be incorporated and function in a nine-membered ring. The experiments were conducted on complexes in a pure state, but in their native membrane. Thus, the protein environment is as near as possible to the native state, an important consideration since this environment can influence carotenoid properties (*4*, *5*). The genetic incorporation of lycopene into LH2 demonstrates that assembly of this complex can occur in the presence of lycopene, and that this new carotenoid has neither altered nor impaired the binding of B800 or B850 bacteriochlorophyll molecules within the complex. The overall efficiencies and pathways of energy transfer from lycopene to the bacteriochlorophylls were determined by fluorescence excitation and ultrafast transient absorption spectroscopies. From the present work and by comparison with previous results, the following general conclusions may be drawn: in LH2, energy is generally transferred from the carotenoids to both B800 and B850, via both the Crt S_2 and S_1 states. The present work provides direct experimental evidence for energy transfer directly from the Crt S_2 state to the BChls, a process which involves the BChl Q_x states as a primary acceptor state.

MATERIALS AND METHODS

Growth Conditions for Rb. sphaeroides. M22+ medium (*20*), supplemented with vitamins, was used for growth of all strains, and liquid cultures were supplemented with 0.1% casamino acids. Antibiotics were used at the following concentrations in μg/mL: 1 (tetracycline); 20 (neomycin); 5 (streptomycin). Transconjugants were grown semiaerobically in the dark on M22+ medium supplemented with antibiotics used at the following concentrations in μg/mL: 1 (tetracycline); 20 (neomycin); 5 (streptomycin), as described in Olsen et al., 1994 (*21*).

Verification of Inactivation of crtC in the LH2-Only Mutants. The LH2-only mutant DPF2 ($LH1^-RC^-$) had been previously constructed by deletion of *pufBALMX* genes and subsequent replacement with a kanamycin resistance cassette (*22*). The plasmid pTC40 is a derivative of the pSUP202 suicide vector containing some of the carotenoid biosynthesis genes with a Tn5 transposon insertion located in the *crtC* gene (*23*). This vector was introduced into DPF2 in order to induce homologous recombination and replacement of the native *crtC* with its transposon-inactivated homologue (Figure 2). Since pTC40 is unable to replicate in *Rb. sphaeroides*, only transconjugant strains whose DNA harbors the transposon will grow on medium containing the appropriate antibiotic. Among the growing colonies, those with a defective *crtC* gene were easily detected by a change in color from red to green. After conjugative transfer, 29 putative *crtC* LH2-only mutants were isolated.

To discard single recombinants in which integration of pSUP202 into the chromosome had occurred, the putative mutants were tested for their ability to grow in the presence of carbenicillin (an ampicillin analogue which is more effective with *Rb. sphaeroides*). Colonies were transferred onto an agar plate with M22+ medium containing this antibiotic and also to a replica plate containing neomycin and streptomycin. Those putative mutants that grew in the presence of carbenicillin were discarded.

A PCR detection method was developed to further identify unwanted single recombinants. The oligonucleotides 5′-GACGCATCGTGGCCGGCATCA-3′ and 3′-GTGGAGCTG-GACTTACCTTCG-5′ were synthesized to serve as forward and reverse primers for PCR. These primers are complementary to a region in the tetracycline resistance gene of pSUP202, which has its origin in pBR322 and should amplify a DNA fragment of 0.95 kb. Two of the mutants that grew in the presence of carbenicillin and a pSUP202 derivative were selected as controls. Reactions were performed in duplicate, and all the positive controls gave a band of the predicted size. Several putative mutants were selected, grown, and further characterized by analyzing their carotenoids by HPLC. In all cases, the only carotenoid present was neurosporene, which confirmed that the desired mutant had been successfully created. As color change is a very effective method of mutant identification (only *crtD* mutants would also appear green, due to the presence of neurosporene and its hydroxy and methoxy derivatives), and given that transposon insertion in *crtC* was encouraged by homologous recombination, further verification was considered unnecessary. The result of these genetic modifications was the construction of a neurosporene-accumulating strain, designated DPF240, that lacked the "core" LH1−RC complex and possessed only the peripheral LH2 complex. This strain was utilized in further experiments to engineer the synthesis of lycopene.

Construction of Strain DPF240[pERWI2] for the Synthesis of Lycopene-Containing LH2 Complex. The *E. herbicola crtI* gene was amplified by PCR and cloned into the broad host range, mobilizable vector pRKSK1 (*24*) to give pERWI2, as described (*25*). pERWI2 was transferred by conjugation into DPF240, to yield strain DPF240[pERWI2].

Pigment Handling, Identification, and Characterization. Carotenoid pigments were extracted using a slightly modified version of the method of Britton and Riesen (*26*), in which cell pellets are dissolved in acetone/methanol 2:1 (v/v) and subsequently transferred into ether. If solvent partition was not achieved, water was added in order to aid the formation of two layers: an upper hydrophobic layer containing the pigments and a lower polar layer with the cell debris. In the few cases when good partition was still not obtained, a few crystals of NaCl were added. The hydrophobic layer was then separated and dried under oxygen-free N_2. Contact of carotenoids with O_2 was avoided at all stages, and their extraction and general handling were carried out in the dark. Carotenoid fractions were either stored in sealed glass vials or used immediately.

Dried carotenoid extracts were dissolved in solvents A and B in the ratio 80:20 (v/v) [A being acetonitrile/water 9:1 (v/v) and B ethyl acetate], which was the starting equilibration buffer. All HPLC solvents were rigorously filtered and degassed. Carotenoids were separated on a Spherisorb ODS2 column (250 × 4.6 mm, i.d.) using a modified protocol provided by Professor A. Young (Liverpool John Moores University, U.K.). The flow rate was constant (1 mL/min), and the elution gradient was the following: 0−6 min, 20−60% B; 6−15 min, 60% B isocratic step; 15−20 min, 60−100% B; 20−20.5 min, 100−20% B; 20.5−30 min, 20% B isocratic step. Most carotenoids were eluted during the isocratic 6−15 min step. Elution was monitored using a Waters 996 photodiode array detector, scanning from 270 to 600 nm every 2 s. Chromatograms at 442 nm were derived from the accumulated absorbance scans using the Millenium software (Waters).

Integration of the carotenoid peaks in the chromatogram was performed at the wavelength corresponding to the absorption maximum (λ_{max}) of each carotenoid, and results are given as percentages of the total sum of the areas.

Preparation of Samples for Spectroscopic Measurements. Cell-free intracytoplasmic membrane (ICM) fractions for use in absorbance spectroscopy were isolated from semi-aerobic cultures of *Rb. sphaeroides* strains using the method of Olsen et al. (*21*). All steps were carried out, as far as possible, at 4 °C. Harvested cells from a 1.5 L culture were resuspended in 20 mL of TE, a few crystals of DNase I were added, and the cells were disrupted in a French pressure cell at 18 000 psi. The broken cells were layered onto a discontinuous (15−40% w/w) sucrose gradient (made up in 1 mM Tris, 1 mM EDTA, pH 7.5), and the gradient was centrifuged in a Beckman Ti45 rotor at 27 000 rpm (57000*g*) for 4 h. The ICM fraction formed a band just above the 15%−40% interface, and was collected with a micropipet. Isolated fractions were stored at −20 °C. The membranes were suspended in 50 mM Tris/HCl buffer, pH 8, for spectroscopy. Pure lycopene was purchased from Sigma and stored in dark at −50 °C. Before experiments, lycopene was dissolved in *n*-hexane to achieve an optical density of about 0.4 at the excitation wavelength. LH2 complexes of wild-type *Rb. sphaeroides* were prepared from the *Rb. sphaeroides* strain 2.4.1 by using the method described by Fraser et al. (*27*). The experiments were performed with the LH2 complexes solubilized in a 20 mM Tris-HCl buffer (pH 8.0).

Fluorescence Spectroscopy. The fluorescence excitation and emission spectra were recorded on a Spex FluoroLOG spectrofluorometer. Absorbance spectra were recorded on a Beckman DU640 spectrophotometer.

Femtosecond Transient Spectroscopy. The femtosecond spectrometer used in these studies is based on an amplified Ti:Sapphire laser system (Spectra Physics), with tunable pulses obtained from optical parametric amplifiers (Light Conversion) or white-light continuum generation. Femtosecond pulses obtained from the Ti:Sapphire oscillator operating at a repetition rate of 82 MHz were amplified by a regenerative Ti:Sapphire amplifier pumped by a Nd:YLF laser operating at a repetition rate of 5 kHz and producing ∼120 fs pulses with an average output power of ∼1 W and a central wavelength of 800 nm. For measurements in the visible range, one part of the amplifier output was used to pump an optical parametric amplifier for generation of the pump pulses, while the other was used to produce white-light continuum probe pulses in a 1 cm sapphire plate. For measurements in the near-infrared region, the amplifier output was divided by a 75/25 beam-splitter to pump two independent parametric amplifiers for generation of the pump and probe pulses. The parametric amplifier used for generation of probe pulses was controlled by a computer, enabling direct scanning of the wavelength of the probe pulses over the spectral region 850−1800 nm. In all experiments, the pump beam was attenuated to ∼20 nJ/pulse and focused to a diameter of ∼500 μm (corresponding to a photon density of $\sim 5 \times 10^{13}$ photons cm^{-2} $pulse^{-1}$). The relative polarization of the pump and probe beams was set to the magic angle (54.7°). An instrument response function of ∼120 fs (fwhm

of a Gaussian fit) was obtained by measuring the cross-correlation of the pump and probe pulses at the sample position, using a 1 mm BBO crystal. Following excitation in the carotenoid spectral region, kinetics were measured at several wavelengths, probing both carotenoid and BChl spectral changes. The measured kinetics were fitted with a sum of exponentials or simulated kinetics based on a kinetic model. By tuning the excitation wavelength to the 0−0 band of the lycopene $S_0 \rightarrow S_2$ transition (525 nm), selective excitation of lycopene was achieved, despite the presence of 20% neurosporene in the sample. All measurements were made in a 2 mm rotating cuvette, and absorption spectra were recorded before and after the transient absorption measurements to check that no degradation had occurred.

RESULTS

Investigation of the Incorporation of Lycopene in an LH2-Only Mutant of Rb. sphaeroides. Previous work has demonstrated that the carotenoid biosynthetic pathway of *Rb. sphaeroides* can be re-routed to produce lycopene (*25*; see also Note Added in Proof). This observation provided further impetus to carry out experiments to alter the carotenoid present in the individual complexes and explore the effect that lycopene would have on membrane-bound LH2 complexes. See Figure 2A for a scheme depicting the effects of the genetic manipulations involved on the carotenoid biosynthetic pathway of *Rb. sphaeroides*. Mutant strains with wild-type carotenoid content capable of synthesizing only LH2 complexes (such as DPF2) were readily available as a result of previous work (*22*). Strain DPF240 was formed from DPF2 by inactivating the *crtC* gene. Plasmid pERWI2, containing the *Erwinia crtI* gene, was introduced by conjugative transfer into mutant DPF240. The subsequent production of a 4-step phytoene desaturase encoded by the *Erwinia crtI* gene allows the biosynthetic pathway to progress from neurosporene (3 desaturations) to lycopene (4 desaturations). The reason that lycopene forms the majority of the carotenoid produced is that several copies of the plasmid-borne 4-step desaturase gene are present, and transcription of this gene is driven by a strong promoter. This tends to override the native 3-step desaturase. Starting with the green mutant DPF240 as recipient, brown-colored transconjugant colonies of DPF240[pERWI2] were obtained, and subsequently used for cell cultures and membrane preparations. The carotenoid content of the mutants was analyzed by HPLC and was found to be 80% lycopene and 20% neurosporene; the chromatograms of DPF240 (green) and DPF240[pERWI2] (brown) can be seen in Figure 2B.

Characterization of the LH2-Only Lycopene-Accumulating Mutant DPF240[pERWI2]. The absorption, fluorescence excitation, and fluorescence emission spectra of DPF240-[pERWI2] membranes can be seen in Figure 3. The absorption spectrum of mutant DPF240[pERWI2] clearly lacked the shoulder at 875 nm associated with LH1, as expected, and possesses peaks at 460, 492, and 525 nm due to the synthesis of lycopene. This new carotenoid seems to be functionally assembled into the LH2 complex, because the fluorescence excitation spectrum shows that energy can be transferred from the lycopene to the bacteriochlorophylls (Figure 3).

It should be pointed out that this strain still contains appreciable quantities of neurosporene. However, both the predominance of lycopene in DPF240[pERWI2] and the clear participation of this carotenoid in energy transfer to the bacteriochlorophylls allow us to conclude that lycopene can join the assembly pathway of the LH2 complex and is functionally integrated into this membrane protein.

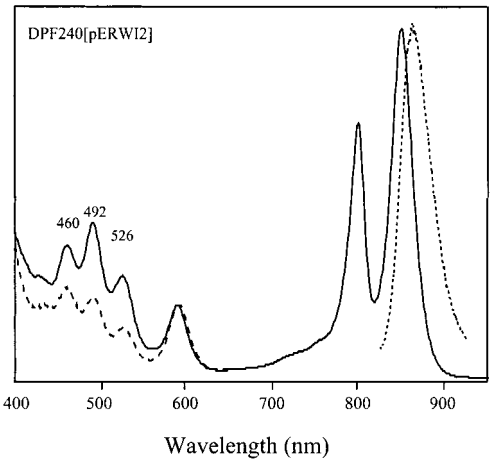

FIGURE 3: Absorption (solid), fluorescence (dotted), and fluorescence excitation (dashed) spectra of *Rb. sphaeroides* containing lycopene (lyco-LH2) at room temperature. The lycopene absorption shows 3 vibrational bands: 0−0 (526 nm), 0−1 (492 nm), and 0−2 (460 nm).

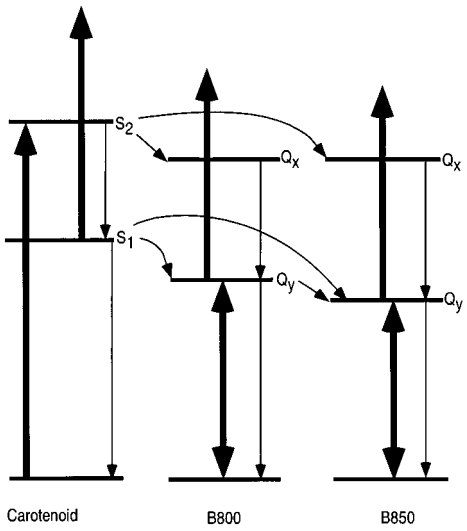

FIGURE 4: Scheme of the energy levels, the probing wavelengths (thick arrows), and the energy-transfer and relaxation processes (thin arrows) which occur between carotenoids and bacteriochlorophylls in LH2.

Femtosecond Transient Absorption Spectroscopy. To further explore the functionality of lycopene in the LH2 complex, we measure ultrafast transient absorption kinetics. We excite the carotenoid S_2 state with a short femtosecond pulse and use the approach of selective probing at many crucial wavelengths corresponding to specific pigments to monitor the ensuing flow of energy throughout the complex. The approach of our pump/probe measurements on lyco-LH2 and WT-LH2 of *Rb. sphaeroides* is illustrated by an energy level diagram involving the first two excited states of the carotenoid and BChl molecules of LH2 (see Figure 4), which is generally used in discussing Crt → BChl energy transfer (*16, 18*). In the scheme, we have indicated excitation and probe processes with solid boldface arrows, while energy-transfer processes are shown with thinner solid

Table 1: Probe Wavelengths (λ_{pr}), Time Constants (τ), and Amplitudes (A) of the Carotenoid to Bacteriochlorophyll Energy-Transfer Processes in LH2 from Wild-Type *Rb. sphaeroides* (WT-LH2) and the Mutant Containing Lycopene (Lyco-LH2) Obtained from a Global Fitting Procedure[a]

	λ_{pr}, nm	τ_1, ps (A_1)	τ_2, ps (A_2)	τ_3, ps (A_3)	τ_4, ps (A_4)	τ_5, ps (A_5)
			Crt S_0-S_2 Bleach			
lyco-LH2	535	0.16 (77%)		3.2 (23%)		
WT-LH2	510	0.17 (80%)		1.7 (20%)		
			Crt S_1-S_n ESA			
lyco-LH2	585	0.16 (−100%)		3.2 (100%)		
WT-LH2	570	0.17 (−100%)	1.7 (82%)	8.0 (12%)		800 (6%)
			B850 ESA			
lyco-LH2	835	0.16 (−54%)	0.8 (−13%)	3.2 (−29%)	15 (15%)	800 (85%)
WT-LH2	840	0.17 (−31%)		1.7 (−50%)	10 (−18%)	800 (100%)
			B850 Bleach			
lyco-LH2	860	0.16 (−34%)	0.8 (−26%)	3.2 (−43%)	15 (21%)	800 (79%)
WT-LH2	890	0.17 (−43%)		1.7 (−55%)	10 (−9%)	800 (100%)

[a] All time constants have an uncertainty of 10%.

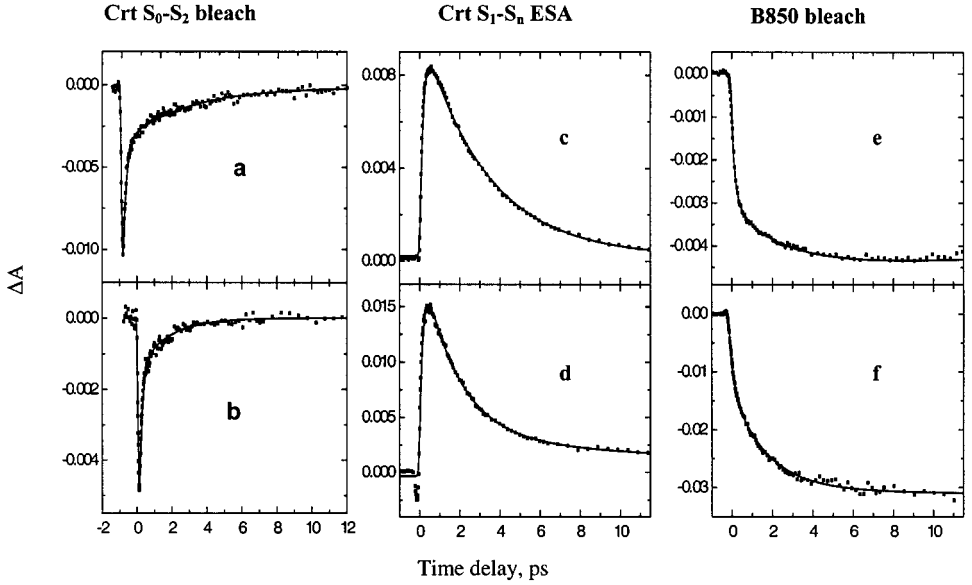

FIGURE 5: Transient absorption kinetics for lyco-LH2 (panels a, c, e) and WT-LH2 (panels b, d, f) at room temperature and at different probing wavelengths (see Table 1). The fits were obtained by convoluting an exponential function with the measured response function (120 fs fwhm).

arrows. Kinetic parameters corresponding to actual physical processes of specific pigment molecules are obtained from individual and global-fitting procedures of data obtained at carefully selected wavelengths. Within experimental error, the results of these two approaches were the same. The results of the global fitting are summarized in Table 1. At wavelengths where multiple transitions are probed, this information can be used as input parameters in a kinetic model. Such an approach is used to analyze our results in the highly congested 800 nm region, revealing new information about the involvement of B800 in the energy transfer from carotenoids. Below we present and discuss our results in detail.

Depopulation of the Crt Donor States (S_2, S_1): Probing Crt $S_0 \rightarrow S_2$ Bleach and $S_1 \rightarrow S_n$ ESA. The ground-state recovery of the carotenoid was probed in lyco-LH2 at 535 nm and the observed kinetics are well described by a biexponential decay with time constants of ∼150 fs and 3.2 ps (see Figure 5a). By probing the Crt $S_1 \rightarrow S_n$ ESA, complementary information is obtained, since this transition also probes the dynamics of the Crt S_2 and S_1 states. Kinetics measured at 585 nm for the lyco-LH2 complex (Figure 5c) are fitted independently and reveal a ∼150 fs rise time and 3.2 ps decay (see Table 1).

In WT-LH2 of *Rb. sphaeroide*s, the $S_0 \rightarrow S_2$ bleaching recovery was probed at 520 nm (Figure 5b) and the $S_1 \rightarrow S_n$ ESA at 568 nm (Figure 5d). Both kinetic traces contain time constants of ∼150 fs and 1.7 ps. It is important to note that the 150 fs time constant obtained by fitting the kinetic data is not determined very precisely in the experiments with ∼120 fs pulses, but independent measurements with better resolution (30 fs pulses centered at 485 nm) yield a more accurate value of 68 ± 10 fs (*28*). Very similar results suggesting sub-100 fs deactivation of the S_2 state were also obtained from fluorescence up-conversion measurements (*15*). In addition, the $S_1 \rightarrow S_n$ kinetics contain a low-amplitude ∼8 ps decay component (see Table 1).

Probing the Dynamics of the B850 Acceptor Pigment. From the energy level scheme of Figure 4, we see that the dynamics of B850 can be probed by its $S_0 \rightarrow Q_y$ (bleaching/SE) or $Q_y \rightarrow S_n$ (ESA) transitions. The two probes are expected to provide very similar information, i.e., the dynamics of the Q_y state, and involve both direct transfer to B850 as well as transfer via B800. For the lyco-LH2

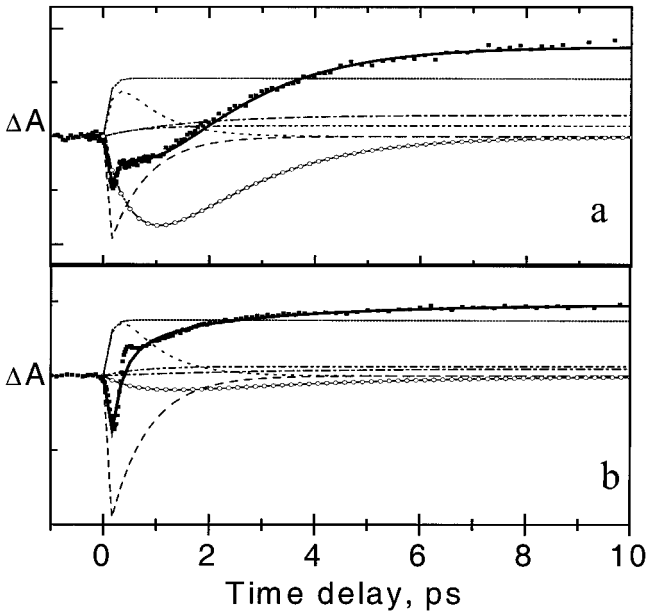

FIGURE 6: Experimental (symbols) and simulated B800 kinetics (thick line) for WT-LH2 (A) and lyco-LH2 (B). The excitation wavelength was 525 nm for lyco-LH2 and 510 nm for WT-LH2. The kinetic components used for simulations were as follows. (A) WT-LH2: B800 ESA (dot; rise = 0.2 ps, decay = 0.7 ps), B800 BL via S_2 (dash; rise = inst., decay = 0.7 ps), B850 ESA via S_1 (dash−dot; rise = 1.7 ps, decay = 800 ps), B850 ESA via B800 (dash−dot−dot; rise = 0.7 ps, decay = 800 ps), B850 ESA via S_2 (short-dash; rise = 0.1 ps, decay = 800 ps), B800 BL via S_1 (line+circles; rise = 0.7 ps, decay = 1.7 ps). (B) Lyco-LH2: B800 ESA (dot; rise = 0.2 ps, decay = 0.7 ps), B800 BL via S_2 (dash; rise = inst., decay = 0.7 ps), B850 ESA via S_1 (dash−dot; rise = 3.2 ps, decay = 800 ps), B850 ESA via B800 (dash−dot−dot; rise = 0.7 ps, decay = 800 ps), B850 ESA via S_2 (short-dash; rise = 0.1 ps, decay = 800 ps), B800 BL via S_1 (line+circles; rise = 0.7 ps, decay = 3.2 ps).

complex, the B850 bleach/SE was probed at 860 nm, and the resulting kinetics are shown in Figure 5e. Contrary to the typical dynamics observed after direct excitation of the B850 band (*29*), the kinetic traces observed here clearly demonstrate additional rise components. To obtain satisfactory fits, three rise components with time constants of ∼150 fs, 800 fs, and 3.2 ps are necessary. The signal decays with time constants of 15 and 800 ps. Very similar time constants were recovered from the measurements probing the Q_y ESA at 835 nm (see Table 1). In WT-LH2, the B850 bleach/SE and Q_y ESA kinetics show two dominant rise times of ∼150 fs and 1.7 ps (Figure 5f). Contrary to lyco-LH2, the 800 fs rise component is not observed in WT-LH2, and another rise component of 10 ps is found with an amplitude of less than 20%. Only one decay component of 800 ps was needed to fit the kinetics in the WT-LH2.

Dynamics of the B800 Intermediate. The spectral region where B800 absorbs and emits light (∼790−830 nm) overlaps strongly with ESA from B850. Furthermore, being an intermediate along the energy-transfer path Crt → B800 → B850 implies that B800 excited states will be populated only very transiently. These factors combine to reveal highly complex kinetics in this spectral region, as shown in Figure 6 for probing at 800 nm. As tested by both global and individual fitting analyses, a conventional fitting procedure in terms of a sum of exponentials will not provide unique solutions in such a complex case. Instead, a kinetic model was developed, based on the energy level diagram in Figure 4. No less than six separate contributions comprise the transient absorption signal at 800 nm. Specifically, we included three components originating from the B800 pigments (fast and slow bleaching due to S_2 and S_1 energy-transfer channels, as well as ESA), and three components arising from ESA of the B850 pigments. Time constants obtained from the carotenoid and B850 spectral regions were taken (Table 1) as fixed input parameters, and the relative amplitudes of each contribution were determined by the modeling. The simulated kinetics are shown in Figure 6, as well as the individual components contributing to the overall response. The implications to the overall energy transfer dynamics in lyco-LH2 and WT-LH2 are discussed below.

Table 2: Lifetime of the Carotenoid S_1 State (τ_{S1}) in Solution[a]

carotenoid, *n*	τ_{S1} (ps)
spheroidene, 10[b]	8.0
lycopene, 11	4.0
lycopene, 11[c]	4.7

[a] All time constants have an uncertainty of 10%. [b] Ref *30*. [c] Ref *10*.

DISCUSSION

In the following, we return to the energy diagram depicted in Figure 4 to analyze the excitation dynamics of the studied *Rb. sphaeroides* lycopene-LH2 (lyco-LH2) mutant and WT-LH2 complexes. A quick glance at this scheme shows that kinetics reflecting energy transfer from the carotenoid to BChl molecules will be highly complex in the general case. The reason for this is the many states involved and the many possible pathways. In addition, several of the transitions indicated in Figure 4 have overlapping spectra. To fully disentangle the web of rate constants and associated amplitudes characterizing this system of coupled pigments and states therefore represents a major challenge. Whether a general energy-transfer pattern exists for various LH2 complexes is not known.

Probing the ground-state bleaching of the Crt $S_0 \rightarrow S_2$ transition in lyco-LH2 shows that two components correspond to the decay: an ∼150 fs component arising from the depopulation of the S_2 state and a 3.2 ps component from the decay of the S_1 state (Table 1). Neglecting other possible contributions to the signal, the 3:1 amplitude ratio between the fast and slow decay components shows that ∼75% of the excitation energy is transferred directly from the Crt S_2 state to B800 and B850, probably via the BChl Q_x states. Of the residual ∼25% which relaxes to the Crt S_1 state, only ∼20% is transferred to B800 and B850 via the Crt S_1 − BChl Q_y pathway, as given by the shortening of the Crt S_1 lifetime from ∼4.0 ps in solution to 3.2 ps in the protein (Table 2). The 4.0 ps S_1 lifetime in solution was obtained from decays of S_0-S_2 bleaching and S_1-S_n ESA of lycopene in *n*-hexane. The estimate of the energy-transfer efficiency from the Crt S_1 state relies on the assumption that the radiationless relaxation rate of the Crt S_1 state in the absence of energy transfer is the same in solution and the protein.

It is interesting to compare the energy transfer via the Crt S_1 pathway in the lyco-LH2 complex to that of LH2 of *Rs. molischianum*. For the latter LH2 complex, a Crt S_1 lifetime of 3.4 ps was obtained. For lycopene in solution, a value of 4.7 ps (*10*) was obtained, showing that the efficiency of energy transfer from Crt S_1 to BChls is very similar in the

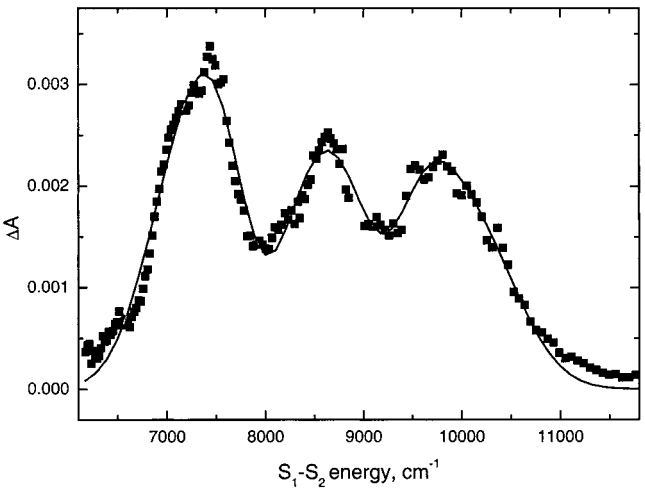

FIGURE 7: S_1-S_2 spectrum of lycopene in *n*-hexane at room temperature. Symbols are experimental data, and the solid curve represents a sum of Gaussians. The excitation wavelength was 505 nm.

two complexes. The differing protein environment in the two complexes has apparently minor importance for the energy transfer; the efficiency is controlled mainly by the photophysical properties of the carotenoid.

In WT-LH2, the deactivation of the Crt S_2 state occurs within 150 fs, and the lifetime of the S_1 state is 1.7 ps. The 4:1 amplitude ratio of the fast and slow decays in the Crt bleaching kinetics suggests that ~80% of the excitations are transferred to the BChls along the direct Crt $S_2 \rightarrow$ B800/B850 channel. The short Crt S_1 lifetime of 1.7 ps, as compared to the 8 ps in *n*-hexane solution (*30*) (see Table 2), shows that the Crt $S_1 \rightarrow$ BChl energy transfer is 80% efficient, in sharp contrast to the only ~20% efficiency of the corresponding process in lyco-LH2 and *Rs. molischianum* LH2 complexes. This result further substantiates previous findings that Crt $S_1 \rightarrow$ BChl energy transfer in LH2 becomes less efficient for carotenoids having 11 or more conjugated double bonds (*10, 17*). Since these results have been obtained for different protein environments, together they strongly suggest that the Crt $S_1 \rightarrow$ BChl energy transfer is controlled by the relative Crt S_1 and BChl Q_y energies. For lycopene, the Crt S_1 energy drops too low to provide efficient coupling to the BChl Q_y states.

Direct measurement of the S_1-S_2 transient absorption spectrum of lycopene in *n*-hexane solution (Figure 7) using the femtosecond IR-probing technique described earlier (*31*) enabled us to determine the S_1 energy by subtracting the S_0-S_2 and S_1-S_2 energies. Using this method, the lycopene S_1 energy was located to 12 500 ± 150 cm^{-1}. This value is ~800 cm^{-1} lower than that obtained from measurements of weak lycopene S_1 fluorescence (*10*), but as described in detail by Polívka et al. (*30*), this discrepancy is most likely due to different carotenoid conformations measured by these two complementary techniques. Since we do not know the conformation of the carotenoid in the LH2 complex, the exact value of the S_1 energy in the LH2 complex will be subject to a large error. However, recent results using femtosecond IR-probing of the S_1-S_2 transition of wild-type LH2 of *Rb. sphaeroides* and *Rps. acidophila* (*32*) show that the S_1 energy of spheroidene in the LH2 complex is similar to that measured in solution, while the S_1 energy of rhodopsin glucoside, having the same conjugated length as lycopene, is slightly red-shifted in the LH2 complex. On the basis of these results, we can safely conclude that the 12 500 cm^{-1} region is an upper limit of the S_1 energy of lycopene in the LH2 complex. Taking into account the expected Stokes shift of ~100 cm^{-1} (*30*), there will be poor spectral overlap between the lycopene S_1 state and the B800 Q_y state (12500 cm^{-1}), and thus slow energy transfer.

To obtain information about the B850 acceptor pigments, kinetics probing the $S_0 \rightarrow Q_y$ SE/bleaching and $Q_y \rightarrow S_n$ ESA regions of the B850 band were used. In lyco-LH2, these kinetics exhibit three rise components: ~150 fs, 800 fs, and 3.2 ps (Table 1). From the measurements probing the Crt bleach and ESA spectral regions and from data on B800 → B850 energy transfer (*12, 33*), we can identify these kinetic components. The very fast ~150 fs rise time of the B850 bleach/SE and ESA correlates to the fast decay of Crt $S_0 \rightarrow S_2$ bleach and equally fast rise of Crt $S_1 \rightarrow S_n$ ESA, providing direct evidence for the Crt $S_2 \rightarrow$ B850 pathway. It has been suggested that this pathway involves a direct Crt $S_2 \rightarrow$ B850 Q_x transfer (*19*), followed by a fast B850 $Q_x \rightarrow Q_y$ internal conversion. However, so far no direct evidence of the involvement of the BChl Q_x state has been demonstrated. As we will show below, the observed kinetic behavior in the B800 band, with delayed onset of B800/B850 ESA, strongly suggests that the B800/B850 Q_x states are transiently populated on the route from Crt S_2 to B800/B850 Q_y. The 3.2 ps B850 rise time correlates to the decay of the Crt S_1 state and shows that this lifetime in fact corresponds to energy transfer via the Crt S_1 channel, and not merely to accelerated Crt $S_1 \rightarrow S_0$ internal conversion. This population time of the B850 excited state most likely includes both direct transfer from the Crt S_1 state and transfer via B800. The presence of an 800 fs rise time component in the B850 dynamics shows that energy is transferred from Crt S_2 to B850 via the B800 Q_y state; the time constant 800 fs is characteristic of B800 $Q_y \rightarrow$ B850 Q_y energy transfer (*12, 33−36*). The presence of the B800 → B850 transfer step implies that a substantial fraction of the energy must be transported via the Crt $S_2 \rightarrow$ B800 $Q_x \rightarrow$ B800 $Q_y \rightarrow$ B850 Q_y pathway. This is also shown by the prompt appearance of B800 bleaching when probing at ~800 nm (see below). The 800 ps decay component is characteristic for the decay of the B850 excited state (*37*). In addition, a lower amplitude ~15−20 ps kinetic component is detected as a decay both in the B850 ESA and in the bleach/SE spectral region.

In WT-LH2, only two rise times (~150 fs and 1.7 ps) are obtained when the dynamics of the B850 are probed. These time constants are clearly resolved, and they correspond to energy transfer via the direct Crt $S_2 \rightarrow$ B850 $Q_x \rightarrow$ B850 Q_y and the indirect Crt $S_2 \rightarrow$ Crt $S_1 \rightarrow$ B850 Q_y channels. A time constant of ~800 fs, signaling substantial Crt $S_2 \rightarrow$ B800→ B850 transfer, is, however, not detected. The reason for this is probably 2-fold: in WT-LH2, the S_1 level of spheroidene is expected to be higher than both the B800 and B850 Q_y states, as known from the S_1 energy in solution (*10, 17, 30*). This leads to the efficient (80%) transfer from the spheroidene S_1 state and a higher amplitude of the 1.7 ps rise time component in the B850 dynamics. Second, the close similarity of the Crt $S_1 \rightarrow$ B800/B850 and B800 → B850 time constants makes it difficult to resolve the ~800 fs B800 → B850 process as a separate time constant.

Table 3: Measured Lifetimes of the S_1 State (τ_{S1}), Time Constants (τ_{ET}), and Efficiencies (ϕ) of Car (S_1) to BChl (Q_y) Energy Transfer[a]

bacterium	carotenoid (*n*)	τ_{S1} (ps)	τ_{ET} (ps)	ϕ (%)
Rb. sphaeroides	spheroidene (10)	1.7	2.1	82
Rb. sphaeroides	lycopene (11)	3.2	16	20
Rs. molischianum[b]	lycopene (11)	3.4	12.3	27

[a] All time constants have an uncertainty of 10%. [b] Ref 10.

Similarly to lyco-LH2, a low-amplitude ~10 ps component is observed in the WT-B850 dynamics. We attribute this feature to a slow-phase energy equilibration within the studied system manifested as a red-shift of the absorption spectrum, which will lead to a rise of the ESA and decay of the bleach/SE at the high-energy side of the transient absorption spectrum, but to a rise of the bleach/SE band at the low-energy side. Depending on the choice of probe wavelength, rise or decay lifetimes will be observed, explaining the different signs of the amplitudes for the WT-LH2 and lyco-LH2 complexes. It is worth noting, however, that no such slow-phase equilibration was observed when the B850 band of wild-type *Rb. sphaeroides* was excited directly (*28*); thus, the presence of this slow equilibration process in the LH2 complexes studied here must be due to excess energy caused by population of Q_x states of BChl. Another source of these equilibration processes could be in principle the presence of carotenoid vibrational relaxation. Very recently, the vibrational relaxation in the S_1 state of carotenoids with 11 conjugated C=C bonds, (lycopene, zeaxanthin, and β-carotene) was measured in solvents with different polarity, yielding 500−800 fs as a time constants of this process (*38*) and thus much faster than the equilibration process observed here.

The results presented above show that the overall efficiency for Crt → B850 energy transfer is ~80% [75% + (25% × 20%)] in lyco-LH2 and ~95% [80% + (20% × 80%)] in WT-LH2 of *Rb. sphaeroides*. The 80% overall efficiency obtained for lyco-LH2 is higher than the value (50%) measured for *Rs. molischianum* LH2 (*10*), while the efficiency of the WT-LH2 agrees with what other authors have reported for the same complex (*18*). The difference in overall Crt → B800/B850 transfer efficiency of lyco-LH2 and WT-LH2 of *Rb. sphaeroides* mainly relates to the low (20%) efficiency of the Crt S_1 → B800/B850 pathway for complexes containing lycopene (see Table 3). If, for simplicity, we assume that all the energy transferred via the Crt S_1 state of lyco-LH2 goes to B850 (5% of the total), and that this fraction is also transferred along this path in WT-LH2, we end up with an ~35:65 ratio of energy transferred from Crt S_1 to B850 and B800 in WT-LH2. This is similar to what was suggested previously (*18*) on the basis of calculations. These results show that in an LH2 complex where the Crt S_1 energy is sufficiently high to provide efficient spectral overlap with both B800 and B850 Q_y states, energy transfer via the Crt S_1 state occurs to both pigments. In the lycopene mutant studied here, in LH2 of *Rs. molischianum* (also containing lycopene), as well as in LH2 of *Rps. acidophila* (containing the carotenoid rhodopsin glucoside, also having 11 conjugated double bonds), the overall efficiency of Crt S_1 → B800/B850 energy transfer is low [20% in lyco-LH2, 27% *in Rs. molischianum* LH2 (*10*), and 28% in *Rps. acidophila* LH2 (*18*)]. The results presented here and the available literature data strongly suggest that a major reason for this behavior is that the S_1 level of carotenoids with 11 or more conjugated double bonds drops too low to efficiently transfer energy to the B800 Q_y state and only the Crt S_1 → B850 channel remains. For carotenoids with even lower S_1 energies, this pathway becomes eventually blocked.

The experimental and simulated B800 kinetics for WT-LH2 and lyco-LH2 shown in Figure 6 are used to further decipher the energy-transfer pathways. The overall appearance of the two measured kinetic curves is quite similar. The most conspicuous feature of the kinetics from both lyco-LH2 and WT-LH2 is the very fast (<100 fs) appearance of B800 bleaching, clearly signaling Crt S_2 → B800 energy transfer. Following this very fast formation of the B800 excited state, there is an equally fast partial decay of the B800 bleaching signal. We do not believe that this recovery is due to fast energy transfer out of B800, but rather represents the growing in of B800 and B850 S_1 → S_n ESA as a result of the ~100 fs BChl Q_x → Q_y internal conversion process along the Crt S_2 → B800/B850 Q_x → B800/B850 Q_y energy-transfer path. This delayed appearance of the B800/B850 S_1 → S_n ESA constitutes direct evidence that the energy transfer from the Crt S_2 state to B800/B850 involves the Q_x state as a primary acceptor state.

From the simulated B800 kinetics shown in Figure 6, it is obvious that for both the lyco-LH2 and WT-LH2 the contributions from B850 constitute approximately 25% of the overall signal. Deconvolving the B800 components, we find the most significant difference between the two samples to be the ratio of signals originating from the carotenoid S_2 and S_1 states. The negative B800 bleach signal arising from energy transfer via the S_1 state is 4 times larger for WT-LH2 than for lyco-LH2, indicating the enhanced efficiency of this channel in the native complex. It is necessary to point out that our simulation of the B800 kinetics does not involve all possible contributions to the B800 signal (e.g., the 10−15 ps equilibration processes observed in the B850 kinetics were omitted). Also, the possible effect of the carotenoid vibrational relaxation mentioned above should be involved in a full picture of the B800 dynamics. However, given the low amplitude of the 10−15 ps time components (Table 1) and also the fact that the carotenoid signals in this spectral region are negligible, the influence of such processes to the simulations of B800 kinetics will be minor. Thus, we conclude that measurements and simulations of both complexes show that B800 is a transient acceptor state in the energy transfer from carotenoids to B850 in LH2.

NOTE ADDED IN PROOF

A full description of the way in which the carotenoid biosynthetic pathway of *Rhodobacter sphaeroides* can be rerouted to produce lycopene and other non-native carotenoids is described in ref *39*, as is the solubilization and purification of a lycopene−LH2 complex. In this complex, lycopene transfers absorbed energy to the bacteriochlorophylls with an efficiency of 54%, which compares favourably with other LH2 complexes containing carotenoids with 11 conjugated double bonds (*39*).

NOTE ADDED AFTER ASAP POSTING

The first sentence of Figure 1 caption has been modified. The version posted on 02/22/02. The correct version was posted 03/19/02.

ACKNOWLEDGMENT

We thank T. Pullerits for valuable discussions and A. Yartsev for technical assistance. We are grateful to R. Cogdell for the generous gift of LH2 complexes of wild-type *Rb. sphaeroides*.

REFERENCES

1. McDermott, G., Prince, S. M., Freer, A. A., Hawthornthwaite-Lawless, A. M., Papiz, M. Z., Cogdell, R. J., and Isaacs, N. W. (1995) *Nature 374*, 517−521.
2. Koepke, J., Hu, X., Muenke, C., Schulten, K., and Michel, H. (1996) *Structure 4*, 581−597.
3. Sundström, V., Pullerits, T., and van Grondelle, R. (1999) *J. Phys. Chem. B 103*, 2327−2346.
4. Fowler, G. J. S., Visschers, R. W., Grief, G. G., van Grondelle, R., and Hunter, C. N. (1992) *Nature 355*, 848−850.
5. Fowler, G. J. S., Hess, S., Pullerits, T., Sundström, V., and Hunter, C. N. (1997) *Biochemistry 36*, 11282−11291.
6. Walz, T., Jamieson, S. J., Bowers, C. M., Bullough, P. A., and Hunter, C. N. (1998) *J. Mol. Biol. 282*, 833−845.
7. Kramer, H. J. M., van Grondelle, R., Hunter, C. N., Westerhuis, W. H. J., and Amesz, J. (1984) *Biochim. Biophys. Acta 765*, 156−165.
8. Van Grondelle, R., Kramer, H. J. M., and Rijgersberg, C. P. (1982) *Biochim. Biophys. Acta 682*, 208−215.
9. Chadwick, B., Zhang, C., Cogdell, R. J., and Frank, H. A. (1987) *Biochim. Biophys. Acta 893*, 444−451.
10. Zhang, J.-P., Fujii, R., Qian, P., Inaba, T., Mizoguchi, T., Koyama, Y., Onaka, K., Watanabe, Y., and Nagae, H. (2000) *J. Phys. Chem. B 104*, 3683−3691.
11. Gillbro, T., and Cogdell, R. J. (1989) *Chem. Phys. Lett. 158*, 312−316.
12. Shreve, A. P., Trautman, J. K., Frank, H. A., Owens, T. G., and Albrecht, A. C. (1991) *Biochim. Biophys. Acta 1058*, 280−288.
13. Trautman, J. K., Shreve, A. P., Violette, C. A., Frank, H. A., Owens, T. G., and Albrecht, A. C. (1990) *Proc. Natl. Acad. Sci. U.S.A. 87*, 215−219.
14. Krueger, B. P., Scholes, G. D., Jimenez, R., and Fleming, G. R. (1997) *J. Phys. Chem. B 102*, 2284−2292.
15. Ricci, M., Bradforth, S. E., Jimenez, R., and Fleming, G. R. (1996) *Chem. Phys. Lett. 259*, 381−390.
16. Andersson, P.-O., Cogdell, R. J., and Gillbro, T. (1996) *Chem. Phys. 210*, 195−210.
17. Desamero, R. Z. B., Chynwat, V., van der Hoef, I., Jansen, F. J., Lugtenburg, J., Gosztola, D., Wasielewski, M. R., Cua, A., Bocian, D. F., and Frank, H. A. (1998) *J. Phys. Chem. B 102*, 8151−8162.
18. Walla, P. J., Linden, P. A., Hsu, C.-P., Scholes G. D., and Fleming G. R. (2000) *Proc. Natl. Acad. Sci. U.S.A. 97*, 10808−10813.
19. Macpherson, A. N., Arellano, J. B., Fraser, N. J., Cogdell, R. J., and Gillbro, T. (2001) *Biophys. J. 80*, 923−930.
20. Hunter, C. N., and Turner, G. (1988) *J. Gen. Microbiol. 134*, 1471−1480.
21. Olsen, J. D., Sockalingum, G. D., Robert, B., and Hunter, C. N. (1994) *Proc. Natl. Acad. Sci. U.S.A. 91*, 7124−7128.
22. Hunter, C. N., McGlynn, P., Ashby, M. K., Burgess, J. G., and Olsen, J. D. (1991) *Mol. Microbiol. 5*, 2649−2661.
23. Coomber, S. A., Chaudhri, M., Connor, A., Britton, G., and Hunter, C. N. (1990) *Mol. Microbiol. 4*, 977−989.
24. Hunter, C. N., Hundle, B. S., Hearst, J. E., Lang, H., Gardiner, A. T., Takaichi, S., and Cogdell, R. J. (1994) *J. Bacteriol. 176*, 3692−3697.
25. Garcia-Asua, G., Lang, H. P., Cogdell, R. J., and Hunter, C. N. (1998) *Trends Plant Sci. 11*, 445−449.
26. Britton, G., and Riesen, R. (1995) in *Carotenoids, Volume 1A: Isolation and Analysis* (Britton, G., Liaaen-Jensen, S., and Pfander, H., Eds.) pp 227−238, Birkhäuser, Basel.
27. Fraser, N. J., Dominy, P. J., Ücker, B., Siminin, I., Scheer, H., and Cogdell, R. J. (1999) *Biochemistry 38*, 9684−9692.
28. Zaushitsyn, Y., Hörvin Billsten, H., and Sundström, V. (unpublished results). This measurement indicates that the 150 fs time constant used in the analysis should be taken as an upper limit for the depopulation of the S_2 state. Although the 30 fs pulses were centered at 485 nm and thus most likely induce additional contributions of S_2 vibrational relaxation, it is clear that the S_2 lifetime is in reality much shorter than 150 fs, as also demonstrated by fluorescence up-conversion (ref *15*).
29. Polivka, T., Pullerits, T., Herek, J. L., and Sundström, V. (2000) *J. Phys. Chem. B 104*, 1088−1096.
30. Polivka, T., Zigmantas, D., Frank, H. A., Bautista, J. A., Herek, J. L., Koyama, Y., Fujii, R., and Sundström, V. (2001) *J. Phys. Chem. B 105*, 1072−1080.
31. Polivka, T., Herek, J. L., Zigmantas, D., Åkerlund, H.-E., and Sundström, V. (1999) *Proc. Natl. Acad. Sci. U.S.A. 96*, 4914−4917.
32. Polivka, T., Zigmantas, D., Herek, J. L., Cogdell, R. J., and Sundström, V. (2002) *Proceedings of Femtochemistry V Conference*, in press.
33. Hess, S., Feldchtein, F., Babin, A., Nurgaleev, I., Pullerits, T., Sergeev, A., and Sundström, V. (1993) *Chem. Phys. Lett. 216*, 247−257.
34. Pullerits, T., Hess, S., Herek, J. L., and Sundström, V. (1997) *J. Phys. Chem. 101*, 10560−10567.
35. Joo, T., Jia, Y., Yu, J. Y., Jonas, D. M., and Fleming, G. R. (1996) *J. Phys. Chem. 100*, 2399−2409.
36. Jimenez, R., Dikshit, S. N., Bradforth, S. E., and Fleming, G. R. (1996) *J. Phys. Chem. 100*, 6825−6834.
37. Bergström, H., Sundström, V., van Grondelle, R., Åkesson, E., and Gillbro, T. (1986) *Biochim. Biophys. Acta 852*, 279−287.
38. Hörvin Billsten, H., Zigmantas, D., Sundström, V., and Polivka, T. (2001) *Chem. Phys. Lett.* (submitted for publication).
39. Garcia-Asua, G., Cogdell, R. J., and Hunter, C. N. (2002) Functional assembly of the foreign carotenoid lycopene into the photosynthetic apparatus of *Rhodobacter sphaeroides* achieved by replacement of the native 3-step phytoene desaturase with its 4-step counterpart from *Erwinia herbicola*. *Mol. Microbiol.* (in press).

BI011741V